

Utah State University

DigitalCommons@USU

International Symposium on Hydraulic Structures

Jun 28th, 1:30 PM - 4:30 PM

Towards a New Design Equation for Piano Key Weirs Discharge Capacity

H. Bashiri

University of Liege, hbashiri@ulg.ac.be

B. Dewals

University of Liege

M. Pirotton

University of Liege

P. Archambeau

University of Liege

S. Epicum

University of Liege

Follow this and additional works at: <https://digitalcommons.usu.edu/ishs>



Part of the [Hydraulic Engineering Commons](#)

Recommended Citation

Bashiri, H., Dewals, B., Pirotton, M., Archambeau, P., Epicum, S. (2016). Towards a New Design Equation for Piano Key Weirs Discharge Capacity. In B. Crookston & B. Tullis (Eds.), *Hydraulic Structures and Water System Management*. 6th IAHR International Symposium on Hydraulic Structures, Portland, OR, 27-30 June (pp. 40-49). 10.15142/T3310628160853 (ISBN 978-1-884575-75-4).

This Event is brought to you for free and open access by the Conferences and Events at DigitalCommons@USU. It has been accepted for inclusion in International Symposium on Hydraulic Structures by an authorized administrator of DigitalCommons@USU. For more information, please contact digitalcommons@usu.edu.



Towards a New Design Equation for Piano Key Weirs Discharge Capacity

H. Bashiri¹, B. Dewals¹, M. Pirotton¹, P. Archambeau¹ and S. Erpicum¹

¹Hydraulics in Environmental and Civil Engineering (HECE)

University of Liege

Belgium

E-mail:

ABSTRACT

Piano Key weirs are Labyrinth-like weirs that can be placed on the top of gravity dams. They represent a powerful solution to increase the discharge capacity of existing dam spillways. For proper design, it is necessary to accurately predict this discharge capacity. In this research, artificial neural network and multiple linear and nonlinear regressions are used to set up a new design equation for the discharge capacity of Piano Key weirs. The effect of each parameter on the discharge capacity of Piano Key weirs is tested in these models. Several non-dimensional parameters are used to define a functional relationship between the inputs and output. These parameters are built from the geometric dimensions of the structure such as weir height, inlet and outlet keys width, overhangs length, water head, and side crest length. Previous experimental data, which were collected at the experimental laboratory of the research group Hydraulics in Environmental and Civil Engineering (HECE), University of Liege, are used for training and testing patterns of the models. Root mean square errors (RMSE) and coefficient of determination (R^2) are used as comparing criteria for the evaluation of the models. The model results compare well with experimental results and other existing equations. They also highlight key geometric parameters governing piano key weirs discharge capacity.

Keywords: Discharge capacity, hydraulic structure, Piano Key weir, artificial neural network, multiple linear regression.

1. INTRODUCTION

The Piano Key weir (PKW) is a modified type of labyrinth weir, which can be placed on the top of gravity dams (Ouamane and Lemperiere 2006). Application of the PKW in reservoirs and rivers has increased in recent years, with projects in France, Vietnam, Sri Lanka, United Kingdom, South Africa, and Australia. The PKW has a complex geometry, and each geometric parameter plays a role on the discharge capacity. The main parameters of PKW geometry are the weir height, the weir unit width, the number of weir units, the side crest length, the inlet and outlet keys widths, the upstream and downstream overhang lengths, and the wall thickness. Figure 1 shows a schematic diagram of a PKW. Various investigations have been done recently on different types of PKWs (Ouamane and Lemperiere 2006; Crookston and Tullis 2010; Machiels et al. 2011; Anderson and Tullis 2012; Leite Ribeiro et al. 2012a; Anderson and Tullis 2013; Machiels et al. 2013; Erpicum et al. 2014).

There are four types of PKWs based on the upstream and downstream overhangs (type A, B, C, and D). According to Figure 2, different types of PKW are described as A) with upstream and downstream overhangs, B) with upstream overhang, C) with downstream overhang, and D) without overhang. Some researchers proposed analytical and numerical equations for calculation of PKW discharge (Leite Ribeiro et al. 2011, 2012b; Kabiri-Samani and Javaheri 2012; Machiels et al. 2014). Leite Ribeiro et al. (2011) applied a non-linear global stepwise regression approach to fit the some dimensionless parameters to propose a mathematical formulation for the PKW. Leite Ribeiro et al. (2012b) investigated the head-discharge relation of A-type PKW experimentally. They showed that relative developed crest length (L/W) and the relative head (P/H) had a significant effect on the discharge capacity. Kabiri-Samani and Javaheri (2012) conducted some experiments to investigate the effect of the PKW geometry on the discharge coefficient for free and submerged flow conditions. They used the classical discharge equation for sharp-crested weirs and proposed an empirical equation for the discharge coefficient for all types of PKWs. Machiels et al. (2014) performed an experimental study to evaluate the influence of the main geometric parameters on the discharge capacity of PKWs. They developed an analytical formula to predict the discharge capacity of the weir. Their

equation is the sum of three components: the discharge per unit length of the upstream crest of the outlet, the discharge per unit length of the downstream crest of the inlet, and the discharge per unit length of the unit length of the lateral crest.

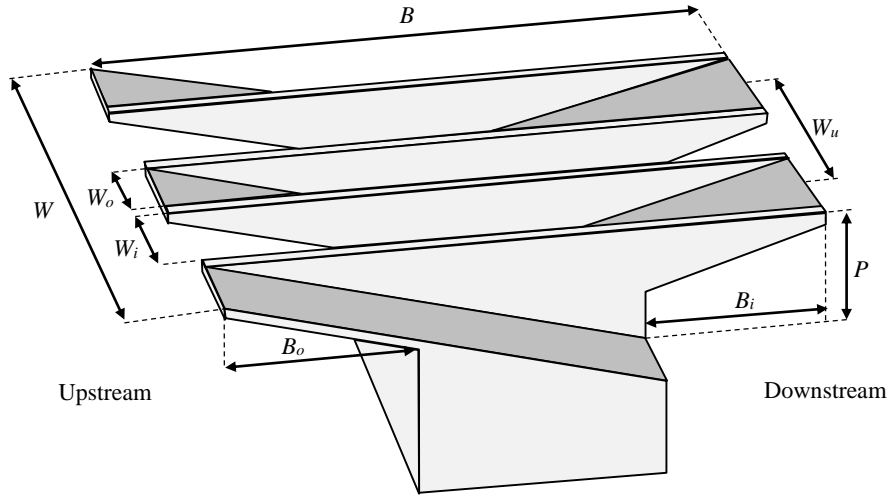


Figure 1. Schematic diagram of a PKW.

The main objectives of the research presented in this paper are to investigate the influence of several geometrical parameters on discharge capacity and to compare the efficiency of some parametrical models to predict the discharge capacity based on basic PKW non-dimensional parameters. Considering the data set of a former study (Machiels et al. 2014), which was collected at the experimental laboratory of the research group Hydraulics in Environmental and Civil Engineering (HECE), University of Liege, different models were tested. In this study, multiple linear regression (MLR), multiple nonlinear regression (MNLr), and artificial neural network (ANN) are applied to develop models for prediction of PKW discharge capacity, and their performance is compared using root mean square error and coefficient of determination. To evaluate the proposed model, we also compared the results with the analytical equation proposed by Leite Ribeiro et al. (2011), Leite Ribeiro et al. (2012b), and Machiels et al. (2014).

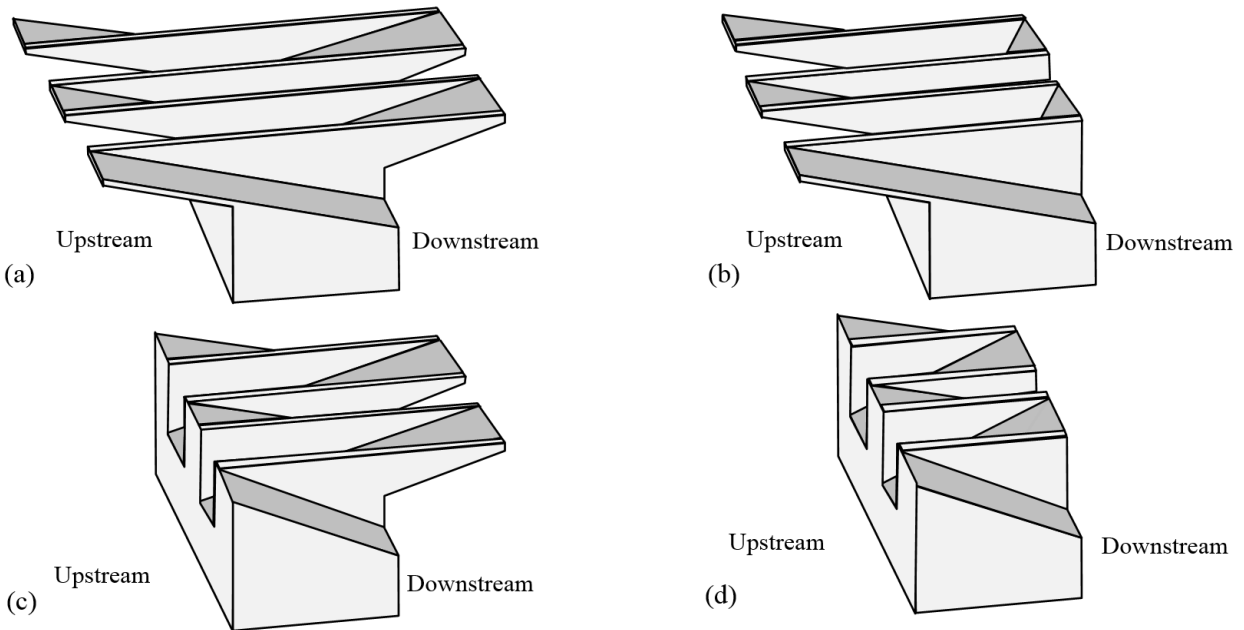


Figure 2. Various types of PKWs: (a) Type A, (b) Type B, (c) Type C, and (d) Type D.

2. METHODS

2.1. Data Set Analysis

The classical discharge equation for a linear free surface weir writes as

$$Q = C_d W \sqrt{2g} H^{3/2} \quad (1)$$

where Q is discharge, g is the acceleration of gravity, H is the total upstream hydraulic head, and W is the weir width. In this study, the non-dimensional discharge coefficient C_d has been investigated based on the discharge per PKW-unit width ($q = Q_u/W_u$). In particular, since this study aims at focusing on the effect of the geometrical parameters of the PKW, different methods have been applied to set up the best function f defined as by the equation below:

$$C_d = f(P/W_u, W_i/W_o, H/P, B/P, B_i/P, B_o/P) \quad (2)$$

where f is the function symbol, P is PKW height, W_i is the inlet key width, W_o is the outlet key width, B_i is downstream overhang length, B_o is upstream overhang length, and B is the side crest length.

Experimental measurements of Machiels et al. (2014) are used as training and testing sets of the MLR, MNLR, and ANN models (1360 tests). The main parameters of their study are listed in Table 1 with their range.

Table 1. Parameter range of PKW in the experiments of Machiels et al. (2014).

Variables	L/W	P/W_u	W_i/W_o	B_o/B_i	H/P	B/P	B_i/P and B_o/P	P_i/P_o
range	5.0	0.33-2	0.46-2.18	0-∞	0.06-3.2	1-6	0-2.67	1

2.2. Multiple Linear Regression

Multiple linear regression (MLR) is a multivariate linear regression method, and its objective is studying the relationship between several independent variables and a dependent variable (Adamowski et al. 2012). The relationship between dependent and independent variables is as follows:

$$y = \alpha_1 x_1 + \alpha_2 x_2 + \dots + \alpha_n x_n + c \quad (3)$$

where α_i are the slopes or coefficients, c is the intercept, n is the number of observations, y is the dependent variable (predicted), and x is the independent variable (observed data set).

2.3. Multiple Nonlinear Regression

Multiple nonlinear regression (MNLR) models show nonlinear relationships between input and output data. There are a lot of mathematical functions for MNLR. The following represents a MNLR equation, which is used in this study.

$$y = \alpha_1 x_1^{\beta_1} + \alpha_2 x_2^{\beta_2} + \dots + \alpha_n x_n^{\beta_n} + c \quad (4)$$

where β_i are additional regression coefficients.

2.4. Artificial Neural Network

The artificial neural network (ANN) is an effective model to predict the output based on input data. The ANN learns any complicated nonlinear function through a training procedure. Many papers show the application and performance of ANN in water resources and hydraulic engineering (Adamowski et al. 2012; Emiroglu and Kisi 2013; Jain 2001). The most applied neural network is the multi-layer perceptron (MLP), which includes layers of parallel perceptrons and is known as a feedforward network. The ANN approach provides an effective way to model data-dependent problems and gives a relationship between input and output data (Araghinejad 2014). Figure 3 shows a typical three-layer feedforward network, known as an MLP. One way to get a good result with an ANN model is to follow up some changes in the number of hidden layer, the number of hidden neurons and transfer function. In this study, we used three-layer perceptrons with a sigmoid activation function (Araghinejad 2014).

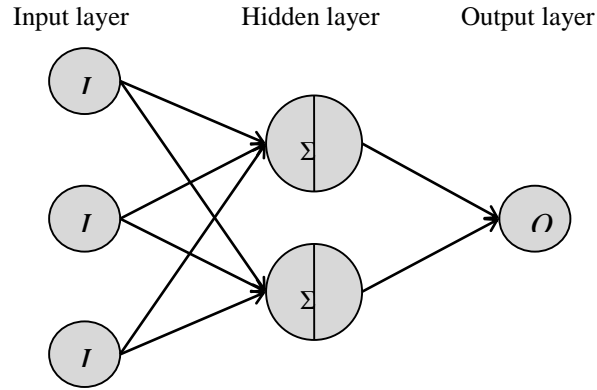


Figure 3. Architecture of a three-layer feedforward network (MLP).

The mathematical equation of MLP approach for calculation of output is (Adamowski et al. 2012)

$$O_k = g_2 \left[\sum_j V_j w_{kj} g_1 \left(\sum_i w_{ji} I_i + w_{j0} \right) + w_{ko} \right] \quad (5)$$

where I_i is input value of node i in the input layer, V_j is the hidden value of node j in the hidden layer, w_{ji} is the weight from input unit i to the hidden unit j , g is the transition function, w_{j0} is the bias for neuron j , w_{kj} is the weight connecting the hidden node j to the output k , w_{k0} is the bias for neuron k , and O_k is the output at node k in the output layer.

2.5. Existing Equations

The results achieved from the best model for each kind of predicting method and their variables are presented in section 3. The predicted results from this study are compared with analytical equations proposed by Leite Ribeiro et al. (2011), Leite Ribeiro et al. (2012b), and Machiels et al. (2014). Leite Ribeiro et al. (2011) applied a non-linear global stepwise regression approach to propose a mathematical formulation for the PKW, as follows:

$$r = \frac{Q_{PKW}}{Q_w} = \frac{C_d L_{eff} \sqrt{2gH^2}^{\frac{3}{2}}}{C_d W \sqrt{2gH^2}^{\frac{3}{2}}} \quad (6)$$

where r is the discharge enhancement ratio between the PKW discharge (Q_{PKW}) and the corresponding rectangular sharp-crested weir discharge (Q_w) and C_d is the discharge coefficient ($C_d = 0.42$). L_{eff} is the effective crest length of the PKW that contributes to the overflow. It is defined as $L_{eff} = N(W_i + W_o + 2T_s + 2B)$ with T_s the side wall width.

$$r = e^{\left(\begin{array}{c} -0.25945 \left(\frac{P}{W_i} \right)^{1.4} \left(\frac{H}{P} \right)^{0.15} + 1.0056 \left(\frac{L}{W_i} \right)^{0.1} \left(\frac{P}{W_i} \right)^{0.5} \left(\frac{H}{P} \right)^{0.7} \\ + 0.067404 \left(\frac{L}{W_i} \right)^{0.3} \left(\frac{P}{W_i} \right)^{0.1} \left(\frac{W_i}{W_o} \right)^{0.25} \left(\frac{H}{P} \right)^{0.2} + 13.9156 \left(\frac{L}{W_i} \right)^{0.35} \left(\frac{H}{P} \right)^{0.15} \\ - 14.0239 \left(\frac{L}{W} \right)^{0.35} \left(\frac{H}{P} \right)^{0.2} + 0.094 \end{array} \right) - 1} \quad (7)$$

Leite Ribeiro et al. (2012b) used a physical based approach to calculate the Q_{PKW} (Eq. (6)). They evaluated the effect of various parameters on Q_{PKW} and divided them into two main groups (primary and secondary parameters). They suggested the equations below for evaluation of the primary effects.

$$\delta = \left(\frac{(L-W)P_i}{WH} \right)^{0.9}; \quad r = 1 + 0.24\delta \quad (8)$$

The effects of the secondary parameters, W_i/W_o , P_o/P_i , $(B_i+B_o)/B$ and R_o/P_o , were considered in the correction factors, as follows:

$$w = \left(\frac{W_i}{W_o} \right)^{0.05}; \quad p = \left(\frac{P_o}{P_i} \right)^{0.25}; \quad b = \left(0.3 + \frac{B_o + B_i}{B} \right)^{-0.5}; \quad a = 1 + \left(\frac{R_o}{P_o} \right)^2 \quad (9)$$

$$r = 1 + 0.24\delta(wpb a) \quad (10)$$

Later, Machiels et al. (2014) suggested that the discharge per PKW-unit width ($q = Q_u/W_u$) can be estimated by following equation:

$$q = q_u \frac{W_o}{W_u} + q_d \frac{W_i}{W_u} + q_s \frac{2B}{W_u} \quad (11)$$

$$q_u = 0.374 \left(1 + \frac{1}{1000H + 1.6} \right) \times \left[1 + 0.5 \left(\frac{H}{H + P_r} \right)^2 \right] \sqrt{2gH^3}; \quad q_d = 0.445 \left(1 + \frac{1}{1000H + 1.6} \right) \times \left[1 + 0.5 \left(\frac{H}{H + P} \right)^2 \right] \sqrt{2gH^3}$$

$$q_s = 0.41 \left(1 + \frac{1}{833H + 1.6} \right) \left[1 + 0.5 \left(\frac{0.833H}{0.833H + P_e} \right)^2 \right] \times \left[\frac{P_e^\alpha + \beta}{(0.833H + P_e)^\alpha + \beta} \right] K_{W_i} K_{W_o} \sqrt{2gH^3}$$

$$P_e = \frac{B_o}{B} P_r + \left(1 - \frac{B_o}{B} \right) \frac{P}{2}; \quad \alpha = \frac{0.7}{S_i^2} - \frac{3.58}{S_i} + 7.55; \quad \beta = 0.029e^{-1.446/S_i}; \quad K_{W_i} = 1 - \frac{\gamma}{\gamma + W_i^2}; \quad \gamma = 0.0037 \left(1 - \frac{W_i}{W_o} \right)$$

$$K_{W_o} = 1 \text{ for } \frac{H}{W_o} \leq \delta_1; \quad K_{W_o} = \frac{2}{(\delta_2 - \delta_1)^3} \left(\frac{H}{W_o} \right)^3 - \frac{3(\delta_2 - \delta_1)}{(\delta_2 - \delta_1)^3} \left(\frac{H}{W_o} \right)^2 + \frac{6\delta_2\delta_1}{(\delta_2 - \delta_1)^3} \left(\frac{H}{W_o} \right) + \frac{\delta_2^2(\delta_2 - 3\delta_1)}{(\delta_2 - \delta_1)^3} \text{ for } \delta_1 \leq \frac{H}{W_o} \leq \delta_2$$

$$K_{W_o} = 0 \text{ for } \delta_2 \leq \frac{H}{W_o}; \quad \delta_1 = -0.788S_0^{-1.88} + 5; \quad \delta_2 = 0.236S_0^{-1.94} + 5$$

(12)

where q_u is the discharge per unit length of the upstream crest of the outlet key, q_d is the discharge per unit length of the downstream crest of the inlet key, q_s is the discharge per unit length of the lateral crest, α and β are the parameters related to the weir geometry, P_e is the mean side wall height, K_{w_i} and K_{w_o} are factors related to the keys width ratio, γ is parameter fitted on the experimental results, and δ_1 and δ_2 are thresholds.

3. RESULTS AND DISCUSSION

3.1. MLR Model

The MLR models for prediction of discharge capacity of PKWs were developed using a spreadsheet software. The MLR models were trained and tested using various combinations of input data. Initially, all the data were selected as input, and the output was predicted. To examine the effect of each parameter on the discharge capacity, we neglect one parameter in each model. For each variable, we used the 1360 data sets. We used two performance indicators, root mean square error (RMSE) and coefficient of determination (R^2), to analyze the different models. In this model, α_1 through α_6 are coefficients of P/W_u , W_i/W_o , H/P , B/P , B_i/P and B_o/P , respectively (Eq. (3)).

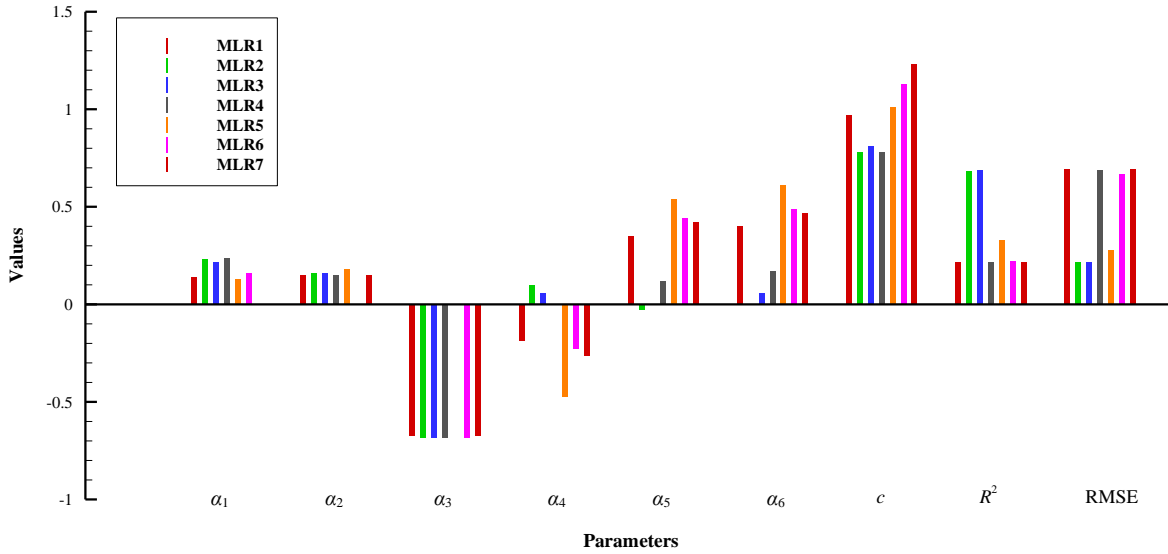


Figure 4. Variables of the MLR models and their performance.

$$R^2 = 1 - \frac{\sum_{i=1}^N (O_i - C_i)^2}{\sum_{i=1}^N (O_i - \bar{O}_i)^2} \quad (13)$$

$$RMSE = \sqrt{\frac{1}{N} \sum_{i=1}^N (O_i - C_i)^2} \quad (14)$$

where N is the number of data set, O_i is the observed data, \bar{O}_i is the average value of observed data, and C_i is the calculated data. Figure 4 shows the different MLR models, their coefficients, and their RMSE and R^2 values. All the models were developed in the same way. Comparison of performance indicators shows that the effect of H/P , B_i/P , and B_o/P on the discharge capacity is more than the other parameters.

3.2. MNLR Model

The MNLR models for prediction of discharge capacity of PKW were developed using a solver function in the spreadsheet software. In this study, we tried to minimize the RMSE for prediction of PKW discharge capacity using Eq. (4). The MNLR model coefficients and their performance is shown in Table 2. The comparison between performance indicators shows that the effect of H/P , P/W_u , W_i/W_o , and B/P on the discharge capacity is more than the other parameters. As it is shown in Table 2, neglecting these parameters has a significant effect on the performance indicators.

3.3. ANN Model

The ANN models were trained and tested based on different combinations of input parameters. The Levenberg-Marquardt backpropagation algorithm was used for neural network training. Among the total data, 70% were randomly selected for training, and the remaining 30% were used for validation and testing. Table 3 shows the values of performance indicators and different combinations of input variables in ANN models. In this study, the hidden layer contains 10 neurons and a tangent sigmoid function was employed as the transfer function. The discharge results for experimental and numerical models using the ANN1 model are compared in Figure 5. The results showed that among the parameters, H/P and W_i/W_o have important effects on the discharge capacity.

Table 2. Variables of the MNLR models and their performance.

Model	Equation	RMSE	R^2
MNLR1	$C_d = 0.22(B_o / P)^{0.51} + 0.08(B_i / P)^{0.88} - 1.89(B / P)^{-0.82} - 4(H / P)^{0.11} + 4(W_i / W_o)^{0.03} + 2.44(P / W_u)^{0.36} - 0.26$	0.1198	0.9050
MNLR2	$C_d = -0.7(B_i / P)^{0.01} - 3.63(B / P)^{-0.45} - 4(H / P)^{0.11} + 4(W_i / W_o)^{0.03} + 4(P / W_u)^{0.26} - 0.22$	0.1193	0.9058
MNLR3	$C_d = 0.09(B_o / P)^{0.53} - 2.54(B / P)^{-0.64} - 3.41(H / P)^{0.13} + 3.16(W_i / W_o)^{0.04} + 2.5(P / W_u)^{0.38} - 0.23$	0.1199	0.9049
MNLR4	$C_d = 1.16(B_o / P)^{0.27} + 1.26(B_i / P)^{0.12} - 3.79(H / P)^{0.12} + 2.21(W_i / W_o)^{0.06} + 4(P / W_u)^{0.07} - 0.37$	0.1349	0.8796
MNLR5	$C_d = -0.69(B_o / P)^{0.05} - 1.02(B_i / P)^{0.05} - 2.83(B / P)^{-0.66} + 0.67(W_i / W_o)^{0.25} + 3.56(P / W_u)^{0.42} + 0.57$	0.3212	0.3181
MNLR6	$C_d = 0.32(B_o / P)^{0.64} + 0.15(B_i / P)^{1.04} - 1.38(B / P)^{-1.09} - 2.85(H / P)^{0.17} + 4(P / W_u)^{0.21} - 0.27$	0.1320	0.8848
MNLR7	$C_d = 1.61(B_o / P)^{0.001} + 1.15(B_i / P)^{-0.004} - 0.4(B / P)^{-2.97} - 4(H / P)^{0.11} + 1.94(W_i / W_o)^{0.08} - 0.25$	0.1366	0.8766

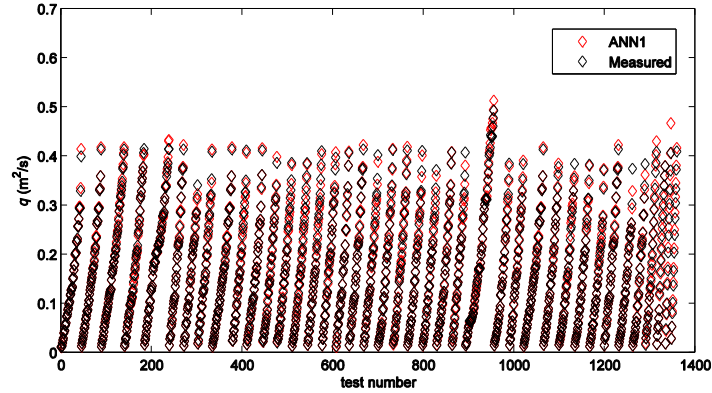


Figure 5. Comparison of predicted versus measured water discharge using the ANN1 model.

3.4. Comparison to Existing Equations

The discharge capacity results using ANN, MNL, Leite Ribeiro et al. (2011), Leite Ribeiro et al. (2012b), and Machiels et al. (2014) are compared with the experimental data (Figure 6). Figure 6 demonstrates that the ANN model with $R^2 = 0.9982$ and RMSE = 0.0046 was found to provide more accurate results than the others.

Table 3. Performance of ANN models.

Model	Input variables	RMSE	R^2
ANN1	$P/W_u, W_i/W_o, H/P, B/P, B_i/P$ and B_o/P	0.0300	0.9940
ANN2	$P/W_u, W_i/W_o, H/P, B/P$ and B_i/P	0.0364	0.9912
ANN3	$P/W_u, W_i/W_o, H/P, B/P$ and B_o/P	0.0380	0.9904
ANN4	$P/W_u, W_i/W_o, H/P, B_i/P$ and B_o/P	0.0353	0.9917
ANN5	$P/W_u, W_i/W_o, B/P, B_i/P$ and B_o/P	0.3182	0.3308
ANN6	$P/W_u, H/P, B/P, B_i/P$ and B_o/P	0.0712	0.9664
ANN7	$W_i/W_o, H/P, B/P, B_i/P$ and B_o/P	0.0377	0.9906

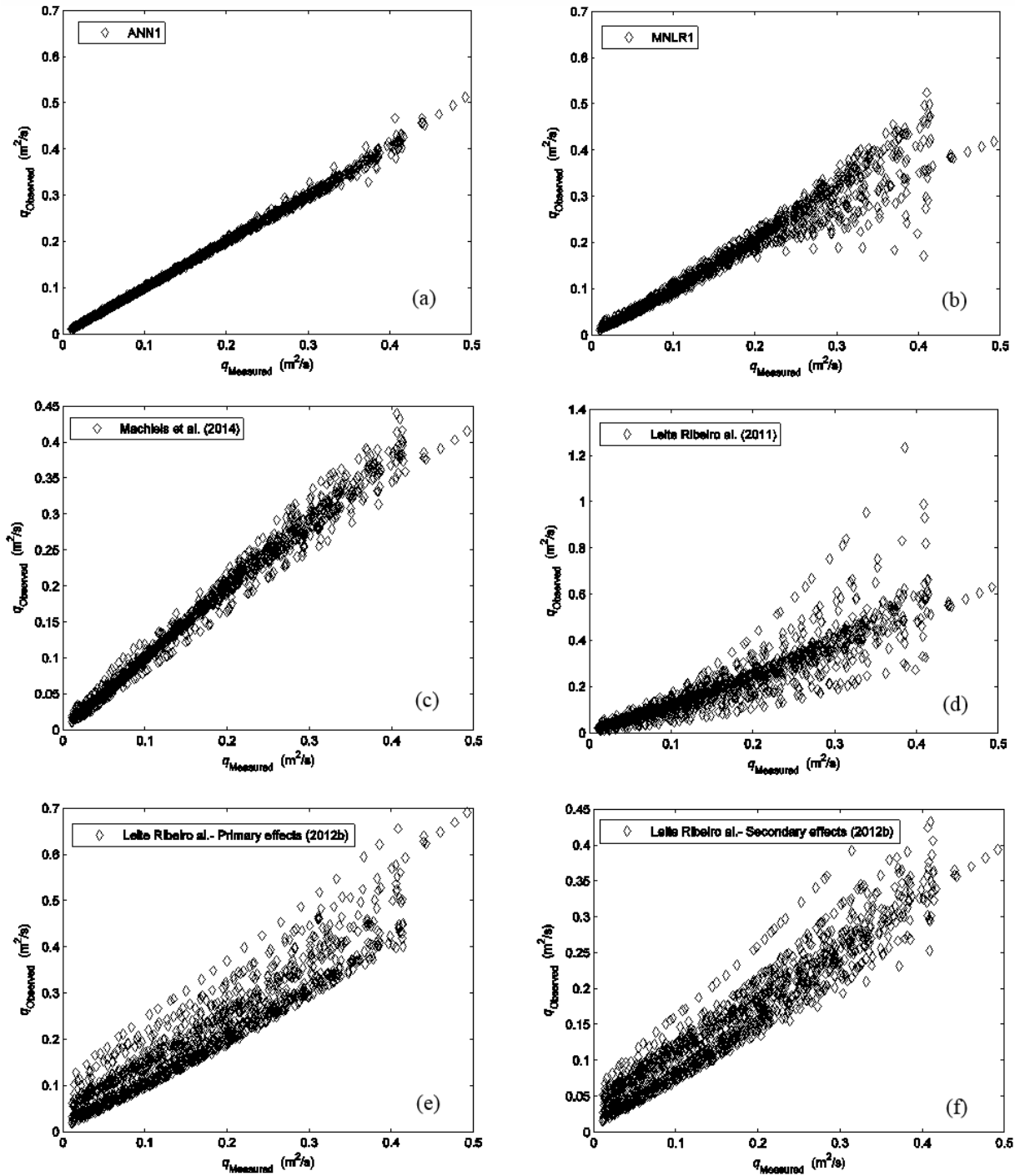


Figure 6. Comparison between measured and computed discharge using (a) ANN, (b) MNLR, (c) Machiels et al. (2014), (d) Leite et al. (2011), (e) Leite et al. (2012b)-Primary effects, and (f) Leite et al. (2012b)-Secondary effects.

4. CONCLUSIONS

Various methods have been applied to set up a predictive equation for PKW discharge capacity considering several non-dimensional geometrical parameters. The measured data for training and comparison were collected at the University of Liege. Existing design equations of Leite Ribeiro et al. (2011), Leite Ribeiro et al. (2012b), and

Machiels et al. (2014) were also considered for comparison. A previous study by Erpicum et al. (2014) highlighted the importance of P/W_u , W_i/W_o , and B_i/B_o . It was determined that H/P , B_i/P and B_o/P are more effective than other parameters in MLR model. Also, H/P , P/W_u , W_i/W_o , and B/P showed significant influence on the discharge capacity in MNLR model. For ANN, it is H/P and W_i/W_o .

Possible future research on prediction of PKWs can include application of other soft computing methods for PKW discharge predicting; evaluation of various analytical equations for the PKW's discharge; and proposing a general and simple equation for all kinds of PKWs using existing data.

5. REFERENCES

- Adamowski, J., Chan, H.F., Prasher, S.O., Ozga-Zielinski, B., and Sliusarieva, A. (2012). "Comparison of multiple linear and nonlinear regression, autoregressive integrated moving average, artificial neural network, and wavelet artificial neural network methods for urban water demand forecasting in Montreal, Canada." *Water Resour. Res.*, 48, W01528, doi:10.1029/2010WR009945.
- Anderson, R.M., and Tullis, B.P. (2012). "Piano Key Weir: reservoir versus channel application." *J. Irrig. Drain. Eng.*, 138(8), 773-776.
- Anderson, R.M., and Tullis, B.P. (2013). "Piano Key Weir hydraulics and labyrinth weir comparison." *J. Irrig. Drain. Eng.*, 139(3), 246-253.
- Araghinejad, S. (2014). *Data-driven modeling: using MATLAB in water resources and environmental engineering*, Springer, Netherlands.
- Crookston, B., and Tullis, B.P. (2010). "Hydraulic performance of labyrinth weirs." *Proc., 3rd International Junior Research and Engineer Workshop on Hydraulic Structures*, Brisbane, Australia, 39-46.
- Emiroglu, M.E., and Kisi, O. (2013). "Prediction of discharge coefficient for trapezoidal labyrinth side weir using a neuro-Fuzzy approach." *Water Resour. Manage.*, 27, 1473-1488.
- Erpicum, S., Archambeau, P., Piroton, M., and Dewals, B.J. (2014). "Geometric parameters influence on Piano Key Weir hydraulic performances." *Proc., 5th Int. Symp. On Hydraulic Structures*, Brisbane, Australia.
- Jain, S.K., (2001). "Development of integrated sediment rating curves using ANNs." *J. Hydraul. Eng.*, 127(1), 30-37.
- Kabiri-Samani, A., and Javaheri, A. (2012). "Discharge coefficients for free and submerged flow over Piano Key Weirs." *J. Hydraul. Res.*, 50(1), 114-120.
- Leite Ribeiro, M., Bieri, M., Boillat, J-L., Schleiss, A.J., Singhal, G., and Sharma, N. (2012a). "Discharge capacity of Piano Key Weirs." *J. Hydraul. Eng.*, 138(2), 199-203.
- Leite Ribeiro, Boillat, J-L., Schleiss, A.J., Doucen, O.L., and Laugier, F. (2011). "Experimental parametric study for hydraulic design of PKWs." *Proc., International Conference on Labyrinth and Piano Key Weirs*, Liege, Belgium, 183-190.
- Leite Ribeiro, M., Pfister, M., Schleiss, A., and Boillat, J-L. (2012b). "Hydraulic design of A-type Piano Key Weirs." *J. Hydraul. Res.*, 50(4), 400-408.
- Machiels, O., Erpicum, S., Dewals, B., Archambeau, P., and Piroton, M. (2011). "Experimental observation of flow characteristics over a Piano Key Weir." *J. Hydraul. Res.*, 49(3), 359-366.
- Machiels, O., Erpicum, S., Archambeau, P., Dewals, B.J., and Piroton, M. (2013). "Parapet wall effect on Piano Key Weirs efficiency." *J. Irrig. Drain. Eng.*, 139(6), 506-511.
- Machiels, O., Piroton, M., Archambeau, P., Dewals, B., and Erpicum, S. (2014). "Experimental parametric study and design of Piano Key Weirs." *J. Hydraul. Res.*, 52(3), 326-335.
- Ouamane, A., and Lemperiere, F. (2006). "Design of a new economic shape of weir." *Proc., Int. Symp. Dams in the Societies of the 21st Century*, Barcelona, CIGB-ICOLD, Paris, 463-470.